

Modeling of hard part machining: effect of insert edge preparation in CBN cutting tools

Tugrul Özel*

Department of Industrial and Systems Engineering, Rutgers, The State University of New Jersey, Piscataway, NJ 08854, USA

Received 17 June 2002; received in revised form 25 October 2002; accepted 10 February 2003

Abstract

High speed machining of hardened steels for manufacturing dies and molds offers various advantages, but the productivity often limited by mainly tool life. This study investigates the influence of edge preparation in cubic boron nitride (CBN) cutting tools on process parameters and tool performance by utilizing practical finite element (FE) simulations and high speed orthogonal cutting tests. The predicted process parameters through FE simulations in high speed orthogonal cutting are expected to help optimize tool life and surface finish in hard machining of AISI H-13 hot work tool steel. A set of orthogonal cutting experiments using honed and chamfered CBN tools was performed and primary cutting force and thrust force were measured by using a force dynamometer along with a PC-based data acquisition system. The same set of cutting conditions was used in numerical FE simulations to predict forces, stresses and temperatures developed at the honed and chamfered CBN tools. Simulation results provided a distribution of stresses and temperatures at the cutting zone, chip–tool and workpiece–tool interfaces. Numerical simulations include testing different edge preparation geometry for CBN tools at different cutting speeds and feeds. The results show that a zone of workpiece material is formed under the chamfer acting as an effective rake angle during cutting. The presence of a chamfer affects the cutting forces and temperatures while no significant change in chip formation observed.

© 2003 Elsevier Science B.V. All rights reserved.

Keywords: CBN cutting tools; Chamfered edge preparation; FE simulations of cutting; Hard part machining

1. Introduction

Traditionally, a wide range of tool steels is used in producing machined dies and molds whereas hot work tool steels (the AISI H series) are generally the choice of material for die-casting and forging dies [1]. AISI H-13 (chromium hot work steel) based dies withstand high process temperatures (315–650 °C) experienced in forging and die-casting and are usually in the hardness of 45–56 HRC [2]. High speed machining of dies and molds in their hardened state replaces the relatively slow electrical discharge machining (EDM) processes in many applications. This approach also reduces the lead-time and the die/mold production costs [1,2]. However, high speed machining of hardened tool steels requires use of advanced cutting tool materials such coated carbides and polycrystalline cubic boron nitride (CBN). CBN tools are suitable for high speed machining of hardened tool steels due to their high hardness, high abrasive wear resistance and chemical stability at high temperatures. CBN cutting tools demonstrate lower strength

becoming more vulnerable for impact load and increased possibility of chipping of the cutting edge.

In high speed machining of hardened steels, increased hardness of the workpiece results in higher than usual cutting forces, stresses and temperatures at the cutting zone. In particular, wear behavior of CBN is highly sensitive to the temperatures developed at the chip–tool and workpiece–tool interfaces (WTIs). Elevated temperatures at the chip–tool interface (CTI), mostly due to friction, cause accelerated diffusion wear in CBN [1]. Thus performance of CBN tools is directly affected by process parameters such as forces, stresses and temperatures at the chip–tool and WTIs.

Predicting stress and temperature distributions using finite element (FE) based numerical simulation of chip formation has the ultimate potential for identifying optimum tool geometry and the cutting conditions. By using this knowledge, tool life and surface finish can be improved in high speed machining of hardened tool steels. Hence, this study aims to investigate the temperatures and stresses developed on the CBN cutting tools with different edge preparations by using a FE based numerical modeling and simulation technique.

Earlier studies for analysis of machining demonstrated that the FE based modeling is the most effective approach to

* Tel.: +1-732-445-1099; fax: +1-732-445-5467.

E-mail address: ozel@rci.rutgers.edu (T. Özel).

obtain detailed temperature and stress distributions on the cutting tools by using commercially available software such as DEFORMTM [3–5] FORGETM [6] and ABAQUS/Explicit [7,8]. In this study, FE models are presented by using the commercial software AdvantEdgeTM [9,10] to simulate high speed orthogonal machining of hardened AISI H-13 tool steel at 55 HRC with honed and chamfered CBN tools.

2. FE modeling of metal cutting

AdvantEdgeTM modeling software is based on a two-dimensional Lagrangian FE model that applies adaptive meshing and continuous remeshing [9]. It assumes that high strain-rate plastic deformations in the workpiece are the result of an unconstrained plastic flow. In the FE model, an orthogonal cutting process in steady state is presented by using the elastic-perfectly plastic workpiece material model and a rigid-perfectly elastic tool body [10].

2.1. Workpiece material modeling

In this study, a material model that has been detailed at the references [9,10] is used. The material model contains deformation hardening; thermal softening and rate sensitivity coupled with a transient heat conduction analysis for finite deformations [10]. A constant friction coefficient of 0.5 was used for the contact at the chip–tool and WTIs.

2.2. FE analysis

FE analysis consisted of 12 simulations using three different cutting speeds (200, 250 and 300 m/min), two different feeds (0.05 and 0.10 mm/rev) and two different

Table 1
Simulation parameters for the FE model

Workpiece material	AISI H-13 (55 HRC)
Tool material	CBN
Workpiece length (mm)	4
Workpiece height (mm)	2
Width of cut (mm)	1
Length of cut (mm)	1.50
Feed (mm/rev)	0.05, 0.10
Rake angle (°)	–5
Clearance angle (°)	5
Flank face length (mm)	0.75
Rake face length (mm)	1

insert edge preparations (honed and chamfered). During the FE simulations, cutting tool initially indents the workpiece, the chip begins to form and finally curls over hitting the workpiece ahead of the cutting zone. In all of the cutting conditions used in this paper, a continuous chip formation is considered for FE simulations. The simulations were performed on a Pentium 400 MHz computer system. Each simulation model required approximately 40 CPU hours of computational time. The simulations were run at the standard steady state analysis mode. FE model for the simulation is shown in Fig. 1 and simulation parameters are given in Table 1.

3. Experiments

3.1. Workpiece specimens and tooling

High speed orthogonal cutting experiments were performed on hardened AISI H-13 tool steel tubes using CBN tool inserts. Steel tubes with 2 mm wall thickness

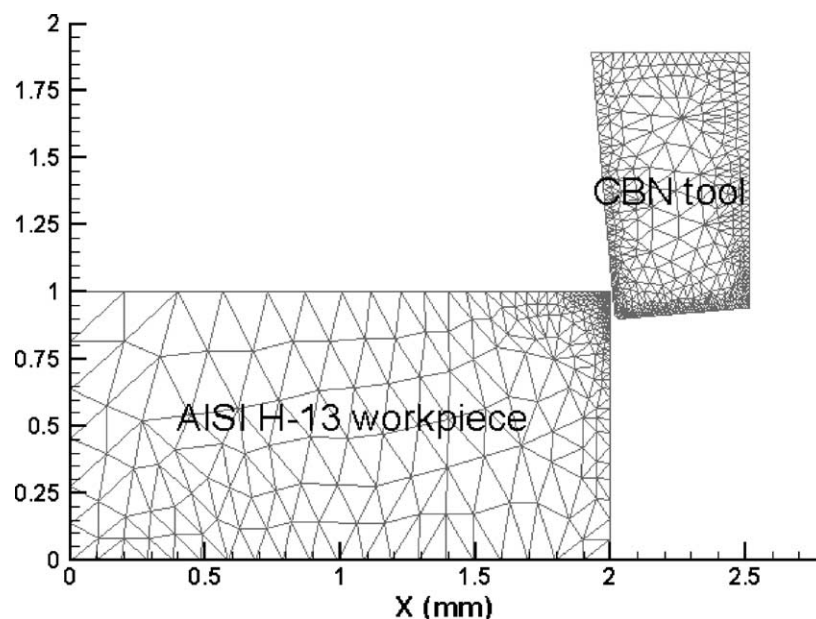


Fig. 1. FE model for the orthogonal cutting.

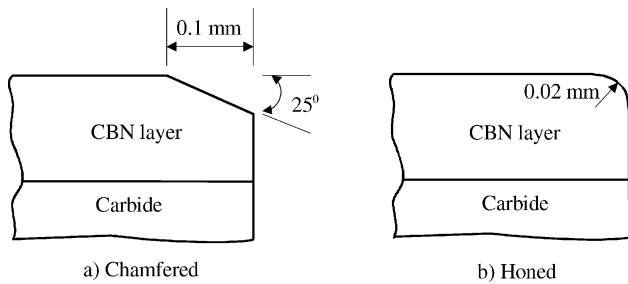


Fig. 2. Edge preparations for the CBN tools.

Table 2
Properties of the CBN material used in experiments

Grain size (μm)	2–4
Binder	TiN
CBN content (%)	70
Knoop hardness (GPa)	28
Transverse rupture strength (GPa)	1
<i>Heat capacity (J/kg K)</i>	
25 ($^{\circ}\text{C}$)	0.507
500 ($^{\circ}\text{C}$)	1.308
Thermal conductivity (W/m K)	100

were cut out of hardened (~ 55 HRC) AISI H-13 cylinder stocks by using wire EDM process at the Laboratories of Engineering Research Center for Net Shape Manufacturing at the Ohio State University. Steel tubes were then turned at a high speed lathe as an end-turning operation creating orthogonal cutting condition is shown in Fig. 3.

3.2. Insert edge preparations for CBN tools

Due to the low mechanical strength of the CBN, cutting edges are generally prepared with a hone radius, or with a chamfer (also called as T land), or with a combination of both. Some of the physical and the mechanical properties of CBN are given in Table 2. Triangular (TNM-433 type) CBN inserts (GE Superabrasives—BZN 8100 grade) with two different edge preparations were used as shown in Fig. 2:

(a) chamfered (chamfer width of 0.1 mm, chamfer angle of 25°), (b) honed (hone radius of 0.02 mm).

3.3. Experimental procedure

In the experiments, the following cutting conditions were used: (a) cutting speed (V) of 200, 250 and 300 m/min, (b) feeds (f) of 0.05 and 0.10 mm/rev. For the force measurement set-up, a tool holder (Kennametal MTCNN-644) that provides negative 5° rake angle and 5° clearance angle was mounted on a three-component piezoelectric force platform (Kistler type 9272) dynamometer. The charge amplifiers (Kistler type 5010) of the force platform were connected to a PC-Pentium based data acquisition system. Accordingly, forces in the principal cutting (F_c) and thrust (F_t) directions were measured.

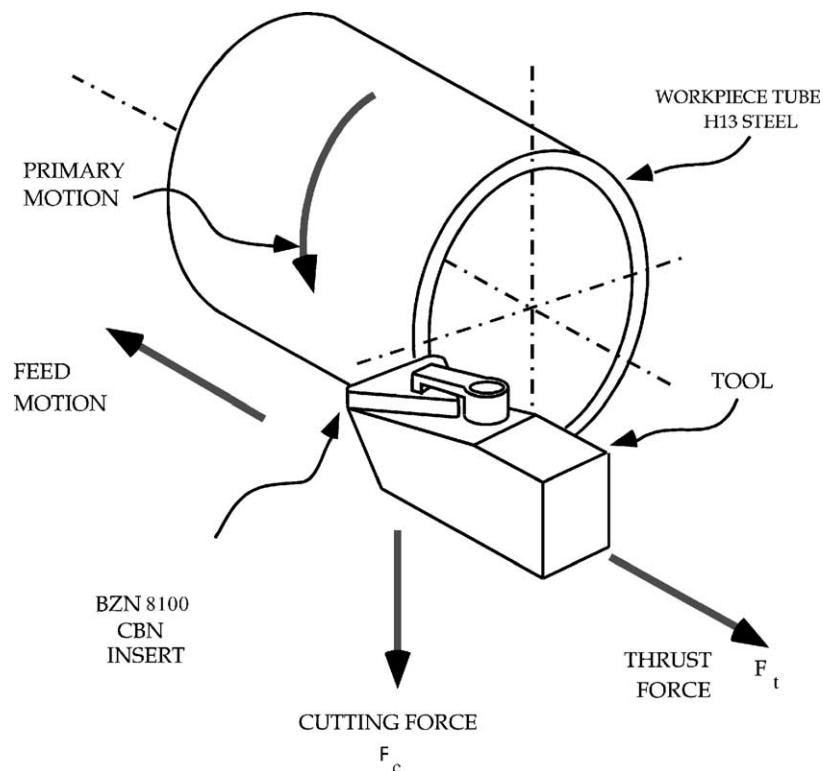


Fig. 3. Illustration of orthogonal cutting experimental set-up.

Table 3
Forces from measurements and simulations for chamfered and honed CBN tools

Insert type	V (m/min)	f (mm/rev)	Measurements		Simulations	
			F _t (N/mm)	F _c (N/mm)	F _t (N/mm)	F _c (N/mm)
Chamfered	200	0.05	180	120	240	240
	250	0.05	220	130	240	240
	300	0.05	180	120	250	220
	200	0.1	220	190	360	310
	250	0.1	230	180	400	320
	300	0.1	240	220	400	325
Honed	200	0.05	180	120	180	140
	250	0.05	150	120	210	170
	300	0.05	180	120	175	135
	200	0.1	230	150	330	170
	250	0.1	230	170	330	175
	300	0.1	230	190	340	175

4. Results

The forces that have been obtained from the measurements and the FE simulations for the cases of using chamfered and honed CBN tools were presented in Table 3. It was found that forces obtained from the simulations showed a similar trend when compared with the experimental ones.

Although, forces obtained from the FE simulations showed reasonable values at the lower cutting speeds, there are substantial differences between the measured and simulated forces at the higher cutting speeds (see Figs. 4 and 5). This may be due to inadequate friction modeling or the limitations in the material model at very large strain-rates. The

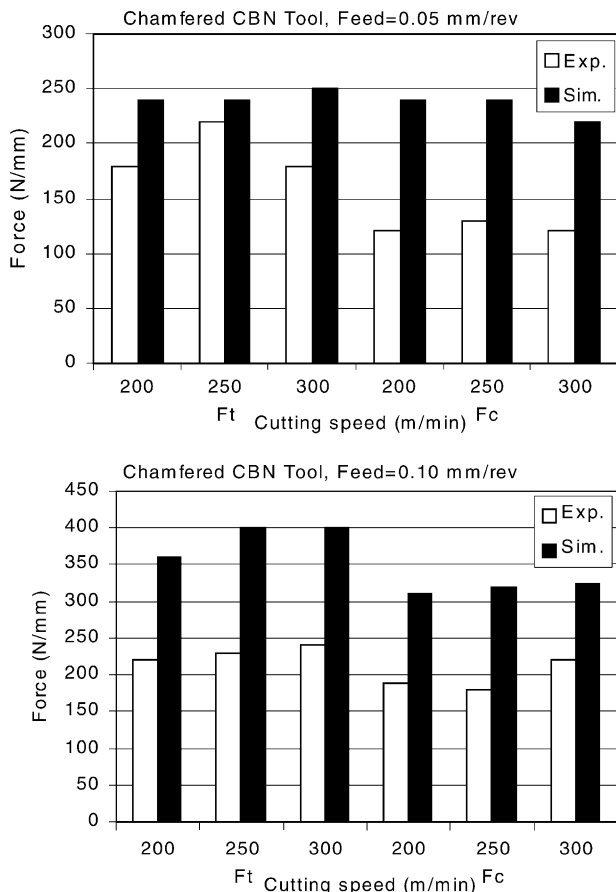


Fig. 4. Comparison of forces for chamfered CBN tool.

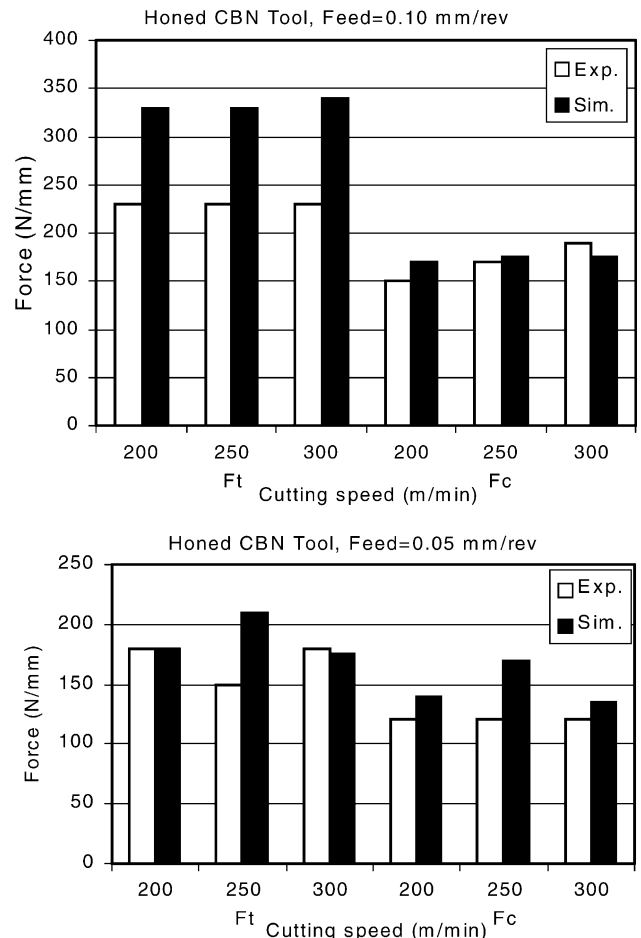


Fig. 5. Comparison of forces for honed CBN tool.

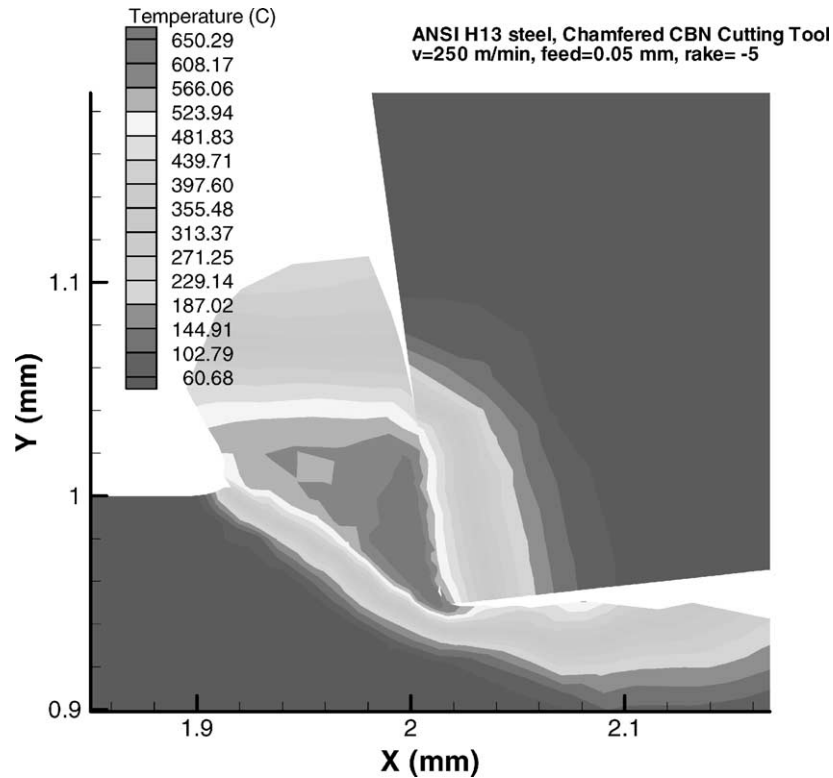


Fig. 6. Temperature distributions on chamfered CBN tools ($V = 250$ m/min, $f = 0.05$ mm/rev).

capabilities of the FEA software allowed only use of an average friction coefficient that was specified as 0.5. The friction generated during machining is more complex indeed and advanced friction models based on CTI conditions are needed [11]. Other researchers also reported similar problems associated with the lack of friction models [5–8]. Simplification in the friction may have resulted in greater simulated force values compared to the experimental data. It is also evident that in the presence of a chamfer, cutting forces are affected highly due to the decreased effective rake angle by the trapped workpiece material under the chamfer geometry [8].

Distribution of temperatures in the workpiece, chip and the CBN tool were obtained from FE simulations of orthogonal cutting is shown in Fig. 6. The temperature generated at the CTI was found substantially higher than the other temperatures. In the FE simulations, maximum temperatures were found between 631 and 807 °C on the tool rake face. The highest temperatures were located on the rake face of the CBN tools and about 0.1–0.15 mm apart from the tool tip in both honed and chamfered edge preparations. Temperatures predicted in other simulations are listed in Table 4. Honed CBN tool geometry resulted in higher values of maximum temperatures than chamfered CBN tool geometry

Table 4
Predicted stresses and temperatures

Insert type	V (m/min)	f (mm/rev)	$ \sigma_x $ (MPa)		$ \sigma_y $ (MPa)		T_{max} (°C)
			CTI	WTI	CTI	WTI	
Chamfered	200	0.05	2618	4789	7066	4828	631
	250	0.05	4130	6583	5313	2104	682
	300	0.05	3222	7540	3835	1630	675
	200	0.10	2158	7267	2467	2183	721
	250	0.10	2843	8131	3403	3390	722
	300	0.10	4717	8760	3744	3679	780
Honed	200	0.05	2589	4921	4812	4264	713
	250	0.05	3930	4977	3533	3404	758
	300	0.05	3727	4351	3535	3292	782
	200	0.10	2269	3170	3343	3003	754
	250	0.10	3509	5324	4119	3958	787
	300	0.10	5744	6821	5104	3812	807

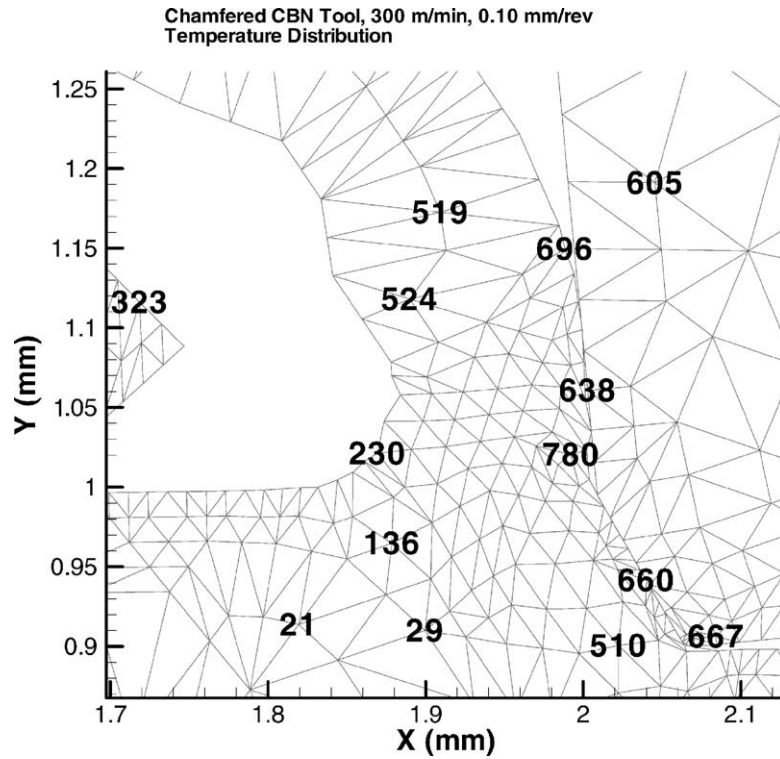


Fig. 7. Nodal temperatures on chamfered CBN tools ($V = 300$ m/min, $f = 0.10$ mm/rev).

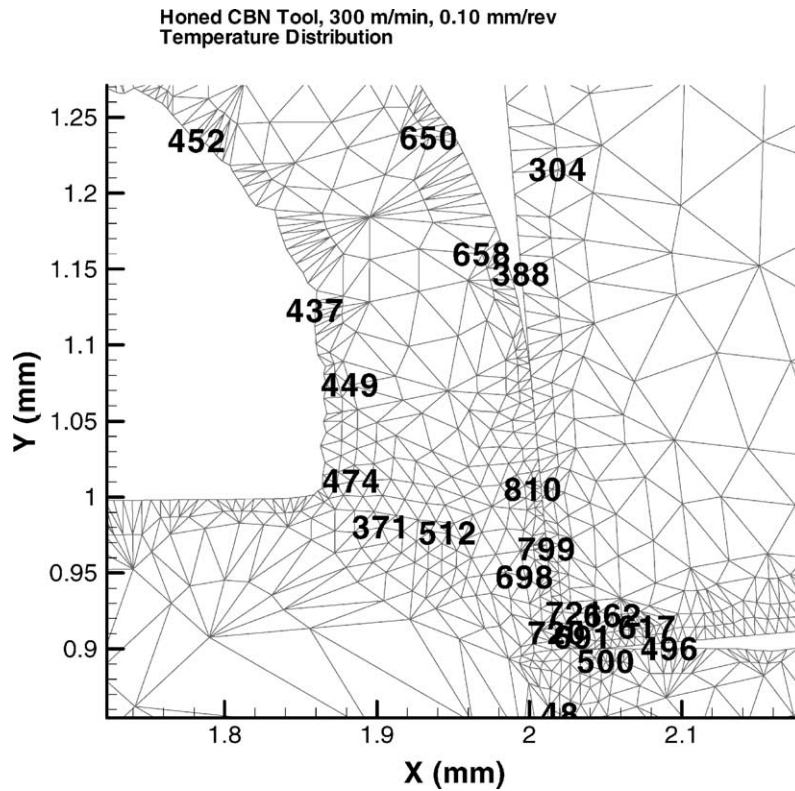


Fig. 8. Nodal temperatures on honed CBN tools ($V = 300$ m/min, $f = 0.10$ mm/rev).

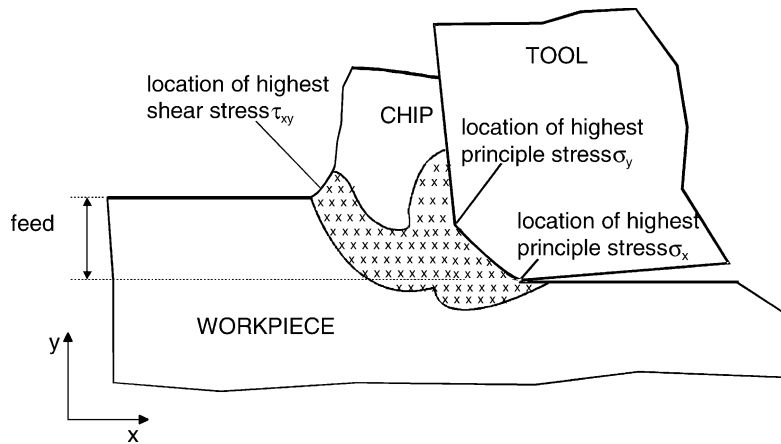


Fig. 9. Locations of maximum stresses in chamfered CBN tools.

during machining. Temperatures generated in the cutting zone and the tool rake face increase, as expected, at higher cutting speeds (see Fig. 6). The detailed temperatures at the nodes of FE model have also been obtained for chamfered and honed CBN tools that are shown in Figs. 7 and 8.

On the rake face of CBN tool, there are locations with high temperature values that are close to threshold values for accelerated crater wear. Furthermore, at high temperatures, abrasive wear resistance of CBN decreases sharply. Therefore, increasing cutting speed is limited by the adverse effect of high temperatures generated at the tool rake face. However, an optimum cutting speed can be identified for a given

feed by analyzing rake face temperatures predicted from FE simulations.

FE simulations reveals not only temperature distributions but also distributions of the all stress components (principal and Von Mises). The stress components in cutting and thrust directions for chamfered and honed CBN tools are shown in Figs. 10–13 at 300 m/min cutting speed and 0.10 mm/rev feed. The nodal stress components showed that generally highest stresses occurred at the lowest feed due to the increase in specific cutting energy [3].

The highest stresses in cutting direction were found at the WTI of the chamfer is shown in Fig. 9. In contrast,

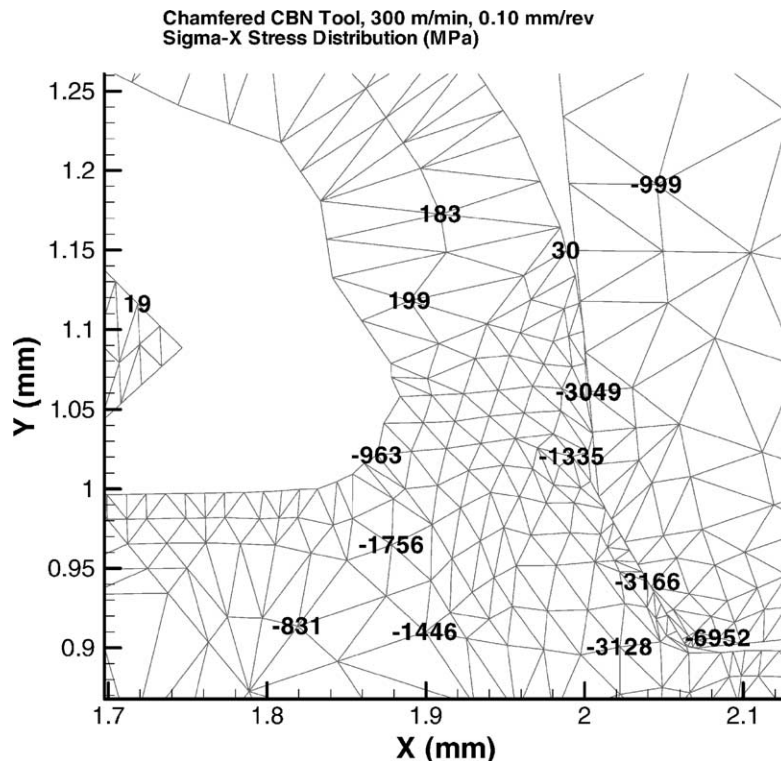


Fig. 10. Nodal σ_x stresses on chamfered CBN tools ($V = 300$ m/min, $f = 0.10$ mm/rev).

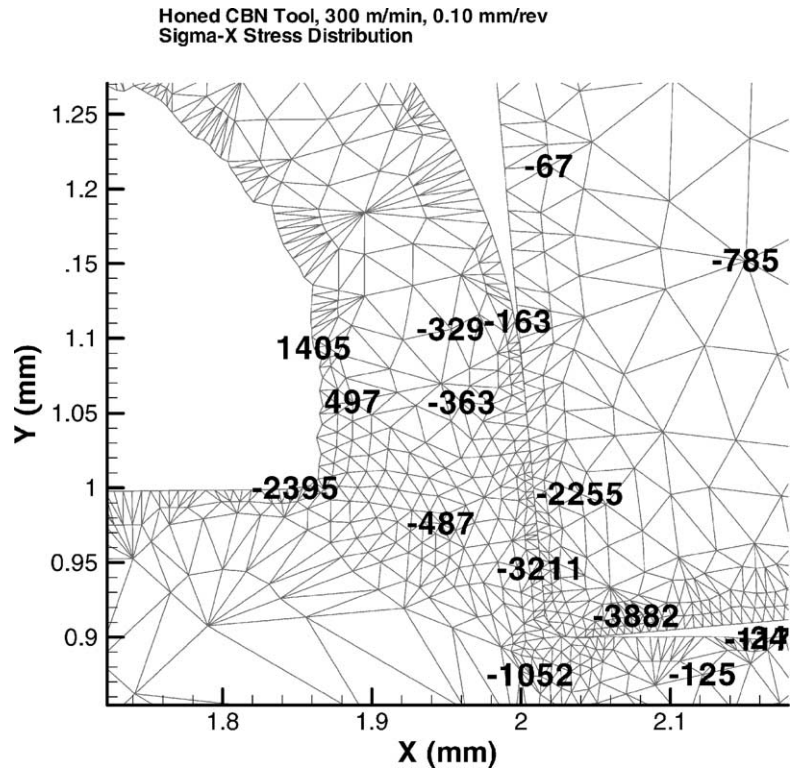


Fig. 11. Nodal σ_y stresses on honed CBN tools ($V = 300$ m/min, $f = 0.10$ mm/rev).

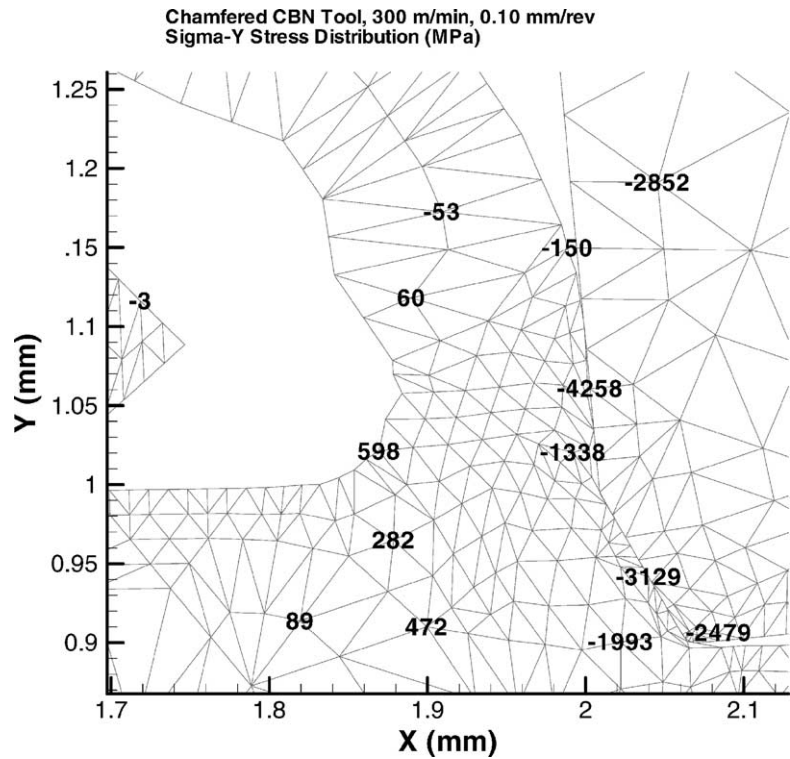


Fig. 12. Nodal σ_y stresses on chamfered CBN tools ($V = 300$ m/min, $f = 0.10$ mm/rev).

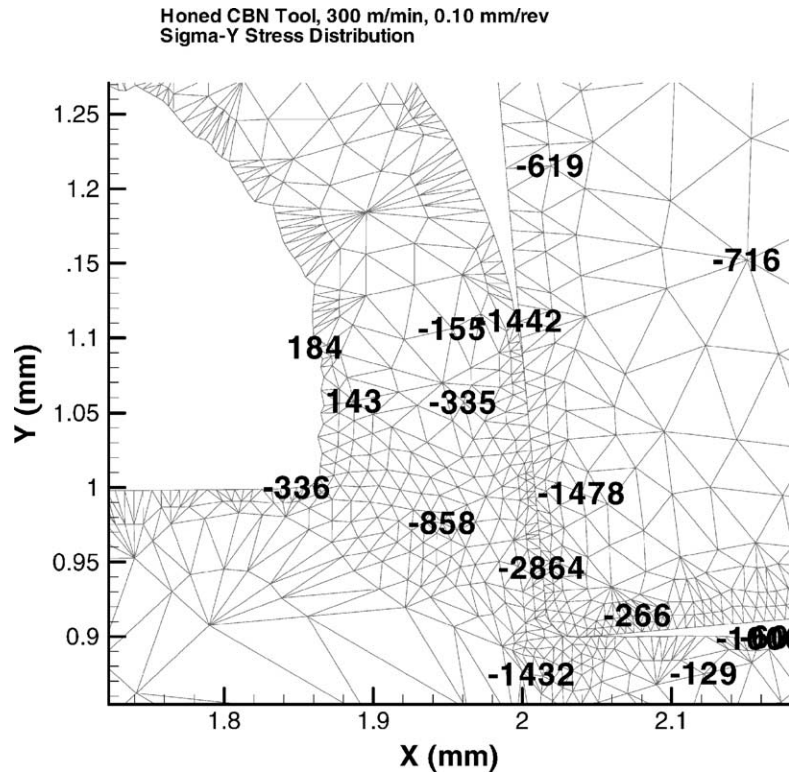


Fig. 13. Nodal σ_y stresses on honed CBN tools ($V = 300$ m/min, $f = 0.10$ mm/rev).

the highest stresses in the thrust direction were identified at the CTI of the chamfer is shown in Table 4. Chamfered CBN tool provided stronger cutting edge to the CBN tool. However, as shown in Table 4, the stress levels are significantly higher at the CTI of the chamfered CBN tool.

5. Conclusions

In this study, the influence of the edge preparation of CBN tools on the process parameters such as forces, stresses and temperatures has been investigated in machining of AISI H-13 tool steel at 55 HRC. The following conclusions can be made:

- An effective rake angle forms in accordance with the trapped workpiece material under the chamfer geometry and highly affects predicted cutting forces.
- Honed CBN tools resulted in lower cutting forces, but higher rake face temperatures.
- Overall, chamfered CBN tools resulted in lower temperatures on the rake face.
- Highest temperatures are at the CTI in about 0.10–0.15 mm distant from the cutting edge.
- The highest stresses in cutting direction were found at the WTI of the chamfered CBN tools.
- The highest stresses in thrust direction were identified at the CTI of the chamfered CBN tools.

- The cutting forces were higher due to the higher thermal conductivity (less thermal softening) of the CBN grade that has been used.

Acknowledgements

The workpiece specimens were prepared at the ERC/NSM of the Ohio State University. The experiments were conducted at Cleveland State University. The author extends his thanks to Paul Bayer and Troy Marusich of Third Wave Systems for the use of AdvantEdge™ software.

References

- [1] P. Fallböhmer, C.A. Rodriguez, T. Özel, T. Altan, High-speed machining of cast iron and alloy steels for die and mold manufacturing, *J. Mater. Process. Technol.* 98 (2000) 104–115.
- [2] R.C. Dewes, D.K. Aspinwall, A review of ultra high speed milling of hardened steels, *J. Mater. Process. Technol.* 69 (1997) 1–17.
- [3] T. Özel, T. Altan, Determination of workpiece flow stress and friction at the chip–tool contact for high-speed cutting, *Int. J. Mach. Tools Manuf.* 40 (2000) 133–152.
- [4] T. Özel, T. Altan, Process simulation using finite element method—prediction of cutting forces, tool stresses and temperatures in high-speed flat end milling, *Int. J. Mach. Tools Manuf.* 40 (2000) 713–738.
- [5] E. Ceretti, M. Lucchi, T. Altan, Finite element simulation of orthogonal cutting: serrated chip formation, *J. Mater. Process. Technol.* 95 (1999) 17–26.
- [6] E.G. Ng, D.K. Aspinwall, D. Brazil, J. Monaghan, Modelling of

- temperature and forces when orthogonally machining hardened steel, *Int. J. Mach. Tools Manuf.* 39 (1999) 885–903.
- [7] Y.B. Guo, C.R. Liu, 3D FEA modeling of hard turning, *ASME J. Manuf. Sci. Eng.* 124 (2002) 189–199.
- [8] M.R. Movahhedy, Y. Altintas, M.S. Gadala, Numerical analysis of cutting with chamfered and blunt tools, *ASME J. Manuf. Sci. Eng.* 124 (2002) 178–188.
- [9] T.D. Marusich, M. Ortiz, Modelling and simulation of high-speed machining, *Int. J. Num. Meth. Eng.* 38 (1995) 3675–3694.
- [10] Theoretical Manual, Third Wave Systems, AdvantEdge™, Version 3.5.
- [11] S. Bhattacharya, M.R. Lovell, Characterization of friction in machining: evaluation of asperity deformation and seizure-based models, *Trans. NAMRI/SME XXVII* (2000) 107–112.